Negative Impedance Technique for Wide Dynamic Range in Radar Systems

[1]AMIR ALMSLMANY, [1]QUNSHENG CAO, [2]CAIYUN WANG
[1]College of Electronic and Information Engineering, [2]College of Astronautics
Nanjing University of Aeronautics & Astronautics
29 Yudao St. - Nanjing - Jiangsu - 210016
CHINA
a.mslmany@nuaa.edu.cn, cao.qunsheng@yahoo.com, wang.caiyun78@yahoo.com

Abstract: - Radar receiver must be able to detect all targets that appears in the designed maximum range, these targets echo signals will have different power levels according to the radar cross section changing, the jamming, and the clutter, this paper proposes a new technique for increasing the wide dynamic range of the radar receiver in order to detect all the signals power levels, this technique based on using time varying gain amplifier (TVGA) for achieving compensation of the power loss due to range, and then using an adaptive sweep optimization (ASO) technique for increasing the linear rejoin of the time varying gain amplifier, the simulation was done using matlab, it shows that intermodulation ratio (IMR) was improved for the time varying gain amplifier electronic circuit, the comparison results with the old methods shows that the probability of detection for the radar was increased using the new technique (ASO/TVGA), for more validation the radar system was tested by detecting three targets at different ranges**.**

Key-Words: - Adaptive Sweep; Amplifier; Detection; Linearity, Time Varying.

1 Introduction

The linearity is an important device parameter for amplifications. In wireless communication systems applications, devices with high linearity can minimize signal distortion, reduce power consumption, and extend battery life. To this end, the research under taken as part of this paper is concerned with the study of improvement of linearity of the time varying gain amplifier (TVGA). For an ideal linear amplifier (LA), the output signal waveform should be directly proportional to the input signal waveform amplitude [1]. In the frequency domain, the spectrum of the output signal and the input signal should have the same frequency components and no additional frequency components will be produced. Linearity enhancement is required when signal contains both amplitude and phase modulation. It can be accomplished either by a chain of LAs or a combination of nonlinear linear amplifiers. Nonlinearities distort the signal being amplified [2].

A recently published work on LAs showed that the nonlinearity can be optimized by tuning the source/load impedance of the baseband and the 2nd harmonic frequency [3], [4]. The traditional nonlinear analysis method using Volterra Series is usually based on a small signal model of transistors [5], while it hardly describes the large signal nonlinearity [6] for the omission of the DC offset with AC input. For some circuits, they have been designed to help radar receivers counteract the effects of external interference and to compensate the power losses, which are involved like as video enhancement features, anti-jamming circuits, or Electronic Counter-Counter Measures (ECCM) circuits. More common video enhancement features associated with radar receivers such as Automatic Gain Control (AGC) were adopted, where the gain control was necessary to adjust the receiver sensitivity for the best reception of signals of widely varying amplitudes. The AGC is not used as frequently as other types of gain control because of the widely varying amplitudes of radar return signals. With the AGC, the gain is controlled by the largest received signals, when several radar signals are being received simultaneously. It is noted that the weakest signal may be of greatest interest [7].

Another enhancement technique is the Instantaneous Automatic Gain Control (IAGC), which is used more frequently than the AGC because it adjusts receiver gain for each signal. The IAGC instantaneously controls the gain of the IF amplifier as the radar return signal changes in amplitude. The range of IAGC is limited, however, by the number of IF stages in which gain is controlled when only one IF stage is controlled, the range of IAGC is limited to approximately 20 dB. If more than IF stages need to be controlled, then

the IAGC range can be increased approximately to be 40 dB [8], [9]. In addition, the Sensitivity Time Control (STC) controls the receiver gain, and it is limited the distance to approximately 50 miles. This is because close-in targets are most likely to saturate the receiver, beyond 50 miles, the STC has no effect on the receiver operates normally [10].

In this work in order to compensate the loss of the received power due to the range, the TVGA technique is introduced, which depends on the idea of the STC circuits , furthermore the TVGA amplifier is used for all ranges of the received echoes power, so it overcomes the drawback of the AGC and no dependent on the number of IF stages so also overcomes the drawback of using the IAGC and also it gives a good results at ranges over 50 miles and then we will apply the adaptive sweep optimization technique for linearity improvement on the TVGA.

By studying of Gummel-Poon model of BJT, the change in the DC component (bias + AC signal DC effect + temperature DC) as a function of both bias and AC input signal for RF linear PAs is theoretically derived, so that the linearity of different DC bias circuits can be interpreted and compared. There are many DC bias circuits, but the most three commonly used DC bias circuits for LPA are namely: the common bias model and the diode bias model and the adaptive bias model [11], [12]. From the comparative results of the mentioned bias types (common bias, diode bias, and the adaptive bias models), it was shown that the diode bias can improve the linearity by decreasing the drop of the DC current I_o. However, the linearity can be more improved, by adding emitter resistance and make optimization to select optimum external circuit elements for the TVGA.

This paper is organized as follows; the second section is to clarify the theoretical analysis of the TVGA, the third section proposes a model of the new ASO/TVGA technique, the fourth section introduces the modeling of the monostatic radar, the echo signal, and the clutter model, in the fifth section the simulation results are demonstrated, and finally the conclusions.

2 Theoretical Analysis of TVGA

The TVGA technique of a monostatic radar system has a predetermined gain versus time relationship. The gain is substantially proportional to the square of the elapsed time measured from the last radar pulse initiating trigger signal. The amplifier consists of a series connection of two amplifiers, each of which has a gain varies linearly with the elapsed time. The idea of TVGA is that, during the receiving time the received echoes in the earlier time will be increased by small voltage gain. On the other hand, the received echoes in the later time will be increased with higher voltage gain so it is clear that the received echoes from the nearest targets (earlier time) will be little increased, however, the received echoes from the farther targets (later time) will be increased more so it will not suffer from the power loss due to long range [13].

As in the ultrasound scan devices, the TVGA works at the same range of frequencies in the radar signal processor at the IF range. Therefore, the TVG technique can be applied on the radar detection exactly in the receiver IF stages to compensate for the range dependent loss.

3 The Previous Model for linearity Enhancement

In order to measure the linearity of TVGA, intermodulation distortion should be measured, by comparing the three models (the common bias, Diode bias, and the adaptive bias), and studying the effect of the circuit elements on the linearity of TVGA, a proposed model for improving the linearity can be introduced. First we will study the analysis of the common bias model, Fig.1 shows the circuit of this model [14].

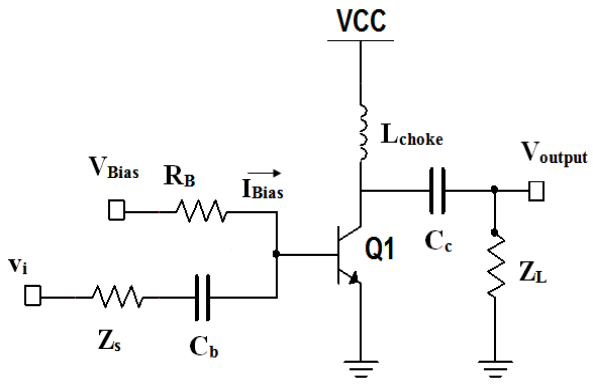

Fig. 1: The common bias circuit for linear amplifier

The 3rd order nonlinear approximation equation of the common bias model is:

$$v_i = V_1(s)\left(\frac{v_{be}}{V_T}\right) + V_2(s)\left(\frac{v_{be}}{V_T}\right)^2 + V_3(s)\left(\frac{v_{be}}{V_T}\right)^3, (1)$$

Where the three input voltages components is in the following equations:

$$V_1(s) = V_T + I_o Z_e + \left[I_o\left(\frac{1}{\beta} + s\tau\right) + sC_{je}V_T\right].$$
$$(Z_i + Z_e) + \frac{sC_{jc}Z_i}{1 + sC_{jc}Z_L}.$$
$$\begin{bmatrix} (1 + sC_{je}Z_e)V_T + \\ I_o\left(1 + \frac{1}{\beta} + s\tau\right)Z_e + I_o Z_L \end{bmatrix}$$

$$= V_T + sC_{je}V_T(Z_i + Z_e) + \frac{sC_{jc}Z_i}{1+sC_{jc}Z_L}.$$
$$(1 + sC_{je}Z_e)V_T + 2V_2(s), \quad (2)$$

Is the first component of the input voltage v_i, and $V_2(s)$is the second component of the input voltage v_i, and equals:

$$V_2(s) = \frac{I_o}{2}\begin{Bmatrix} Z_e + \left(\frac{1}{\beta} + s\tau\right)(Z_i + Z_e) + \\ \frac{I_o}{2}\frac{sC_{jc}Z_i}{1+sC_{jc}Z_L}\left[Z_L + \left(1 + \frac{1}{\beta} + s\tau\right)Z_e\right] \end{Bmatrix}, \quad (3)$$

$$V_3(s) = \frac{I_o}{6}\begin{Bmatrix} Z_e + \left(\frac{1}{\beta} + s\tau\right)(Z_i + Z_e) + \\ \frac{I_o}{6}\frac{sC_{jc}Z_i}{1+sC_{jc}Z_L}\left[Z_L + \left(1 + \frac{1}{\beta} + s\tau\right)Z_e\right] \end{Bmatrix}$$
$$= \frac{1}{3}V_2(s), \quad (4)$$

Is the third component of the input voltage v_i, as $\beta = 100$ then make these approximations:

$$\left(\frac{1}{\beta} + s\tau\right) = s\tau, \quad \left(1 + \frac{1}{\beta} + s\tau\right) \cong (1 + s\tau)$$

Rewrite equations (2), (3), and (4):

$$V_1(s) = V_T + I_o Z_e + \left[I_o s\tau + sC_{je}V_T\right](Z_i + Z_e) + \frac{sC_{jc}Z_i}{1+sC_{jc}Z_L}\begin{bmatrix} (1 + sC_{je}Z_e)V_T + \\ I_o(1 + s\tau)Z_e + I_o Z_L \end{bmatrix}$$
$$= V_T + sC_{je}V_T(Z_i + Z_e) + \frac{sC_{jc}Z_i}{1+sC_{jc}Z_L}(1 + sC_{je}Z_e)V_T + 2V_2(s) \quad (5)$$

$$V_2(s) = \frac{I_o}{2}Z_e + \frac{I_o}{2}s\tau(Z_i + Z_e) + \frac{I_o}{2}\frac{sC_{jc}Z_i}{1+sC_{jc}Z_L}[Z_L + (1 + s\tau)Z_e], \quad (6)$$

$$V_3(s) = \frac{I_o}{6}Z_e + \frac{I_o}{6}s\tau(Z_i + Z_e) + \frac{I_o}{6}\frac{sC_{jc}Z_i}{1+sC_{jc}Z_L}[Z_L + (1 + s\tau)Z_e]$$
$$= \frac{1}{3}V_2(s) \quad (7)$$

Considering equations (5), (6), and (7) it is worthy to note the existence of intrinsic and extrinsic time constants $(\tau, C_{jc}Z_i, C_{jc}Z_L, and\ C_{je}Z_e)$ respectively that can be used for normalization of the form $\omega_n = 1/\tau$, these voltage components are function of operating frequency. Studying the effect of the circuit extrinsic elements of this model on the voltage components as a function of frequency it is possible to know how these elements can affect the linearity of the TVGA. The voltage $V_1(s)$ is the most important component in the linearity measurements, so the following studies will concern $V_1(s)$.

3.1 The Extrinsic Elements Effects

By studying the variation of $V_1(s)$as a function of operating frequency with the input source impedance Z_S, the voltage $V_1(s)$will increase as the input impedance increases, and the same result will happen when we study the variation of $V_1(s)$ with the load impedance Z_L, the choke coil L_{choke}, and the emitter resistance R_e, but in the case of the emitter resistance R_e we get the best results comparing with the other components.

3.2 The Intrinsic Elements Effects

By studying the variation of $V_1(s)$as a function of operating frequency with the output junction capacitance C_{jc} , the voltage $V_1(s)$will increase as the output junction capacitance increases, and the same results will happen when we study the variation of $V_1(s)$ with the diffusion capacitance C_d, but in the case of the emitter resistance R_e we get the best results comparing with the other components. Comparing these results, it can be seen that the emitter resistance has the great effect on the voltage $V_1(s)$, so it will give the best results in improving the linearity of the TVGA.

3.3 The Proposed Model Analysis

As proved above the linearity of the TVGA can be improved using extrinsic parameters of the amplifier circuit by adding an emitter resistance, such that:

$$R_B \ll \beta R_e \quad (8)$$

Fig.2 shows the circuit of the proposed model. The analysis shows that the output signal consists of AC components, DC components, and other intermodulation components that appears when the input is composed of two adjacent tones.

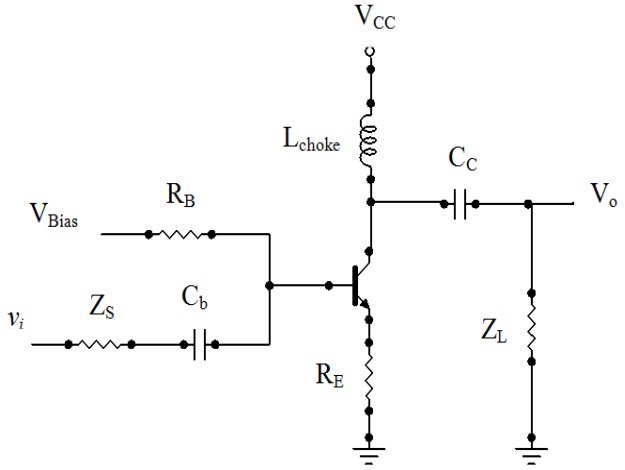

Fig. 2: The circuit of the proposed model

Fig.3 shows the equivalent circuit of the proposed model including the emitter resistance, and the transistor internal equivalent circuit. Note that the emitter junction capacitor is neglected since: $C_d \gg C_{je}$ by making AC analysis and DC analysis it can be seen that:

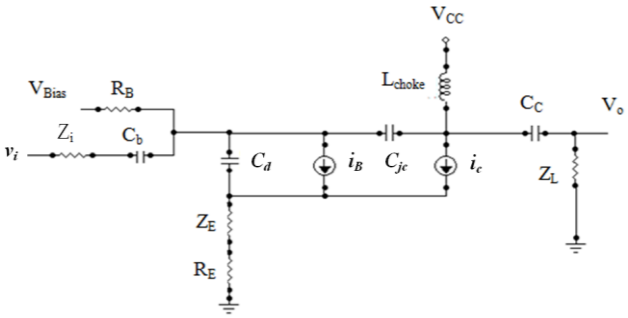

Fig. 3: The equivalent circuit of the proposed model

$$V_1(s) = V_T + I_o\left(r'_e + R_e\right) + I_o s\tau.\left(Z_i + r'_e + R_e\right) + \frac{sC_{jc}Z_i}{1+sC_{jc}Z_L}.$$

$$\left[V_T + I_o(1+s\tau)\left(r'_e + R_e\right) + I_o Z_L\right]$$

$$= V_T + \frac{sC_{jc}Z_i}{1+sC_{jc}Z_L}V_T + 2V_2(s), \quad (9)$$

$$V_2(s) = \frac{I_o}{2}\left\{\begin{array}{l}\left(r'_e + R_e\right) + s\tau\left(Z_i + r'_e + R_e\right) + \\ \frac{sC_{jc}Z_i}{1+sC_{jc}Z_L}\left[Z_L + (1+s\tau)\left(r'_e + R_e\right)\right]\end{array}\right\}, \quad (10)$$

$$V_3(s) = \frac{I_o}{6}\left\{\begin{array}{l}\left(r'_e + R_e\right) + s\tau\left(Z_i + r'_e + R_e\right) + \\ \frac{sC_{jc}Z_i}{1+sC_{jc}Z_L}\left[Z_L + (1+s\tau)\left(r'_e + R_e\right)\right]\end{array}\right\}$$

$$= \frac{1}{3}V_2(s) \quad (11)$$

The DC equation will be:

$$I_o \approx \frac{I_{oq}}{1+Kv_{sm}{}^2} \approx I_{oq}(1 - Kv_{sm}{}^2) = I_{oq}\left[1 - \frac{1}{2}\left(\frac{v_{sm}}{V_1(s)}\right)^2\right] \quad (12)$$

$$|\mathrm{IMR3}| = \left|\frac{3}{4}\frac{\mathrm{F_3(S_1, S_1, -S_2)}}{\mathrm{F_1(s_1)}}\right|\left|\frac{\mathrm{V_{sm}}}{\sqrt{2}}\right|^2 = \frac{3|\mathrm{V_{sm}}|^2}{8}f_1(I_o) \quad (13)$$

4 Monostatic radar and signal modelling

In order to simulate a complete monostatic pulse radar model, the environment conditions such as ground clutter (log normal distribution), and noise (AWGN) must be considered. Because the coherent detection requires phase information and more computationally expensive, we assume that the pulsed radar system we will use a non-coherent detection scheme. We choose a linear frequency modulated (LFM) waveform in this model. The desired range resolution determines the bandwidth of the LFM waveform which will determines the pulse width [15-17]. Another important parameter of a pulse waveform is the pulse repetition frequency (PRF). The PRF is determined by the maximum unambiguous range [18], [19].

The power of the thermal noise is related to the receiver bandwidth. The receiver's noise bandwidth is set to be the same as the bandwidth of the waveform, which is often the case in real systems. In order to model the transmitter we must calculate the peak transmitted power. The required peak power is related to many factors including the maximum unambiguous range, the required SNR at the receiver, and the pulse width of the waveform.

Among these factors, the required Signal to Noise Ratio (SNR) at the receiver is determined by the design goal of P_D and P_{FA}, as well as the detection scheme implemented at the receiver. For the non-coherent detection scheme, the calculation of the required SNR is, in theory, quite complex. Fortunately, there are good approximations available, such as Albersheim's equation [20], in which the required SNR can be derived as:

$$SNR=-5\log_{10}N+\left[6.2+\left(\frac{4.54}{\sqrt{N+0.44}}\right)\right]\log_{10}(A+0.12AB+1.7B), \quad (13)$$

where N is the number of pulses,

$$A=\ln\left(\frac{0.62}{P_{FA}}\right), \quad B=\ln\left(\frac{P_D}{1-P_D}\right)$$

Once the required SNR has been obtained at the receiver, the peak power at the transmitter can be calculated using the radar equation given by the follow equation:

$$P_T=\left(\frac{RG_TG_R\lambda^2\sigma}{(4\pi)^3(SNR)kT_\circ BF_nL}\right)^{1/4}, \quad (14)$$

where P_T is the transmitted peak power, G_T, G_R are the transmitter and the receiver gain, respectively. λ is the wavelength and σ is the radar cross section area, and k is the Boltzmann's constant 1.38×10-23 (Watt*sec/°Kelvin), and T is the temperature 290 K, and B is the receiver band width, and F_n is the receiver noise figure, and L is the loss factor. From (14) the resulting power is about 1.7 KW, which is very reasonable. In comparison, the resulting peak power would be 3.5 KW if had not used the pulse integration technique, with all this information, we can configure the transmitter [21]. Also we must introduce the surface clutter into the simulation to ensure the system can overcome the effects of surface clutter [22].

The TVGA is located after matched filter. In radar applications, the threshold has been often chosen so that the P_{FA} is below a certain level. In our model, the white Gaussian noise and non-coherent detection have been selected. The signal power threshold is given by,

$$T=-\beta^2\ln P_{FA}, \quad (15)$$

where β^2 is the total noise power.

In the block diagram the matched filter offers a processing gain which improves the detection threshold. After the matched filter stage, the SNR is improved. However, because the received signal power is dependent on the range, the return power from a target is still much stronger than the power farther away it.

From probability theory we know that the probability of detection for single radar can be calculated from:

$$P_d=\int_T^\infty P(v)\,dv, \quad (16)$$

where P(ν) is the probability density of the power of IF target signal plus noise and T is the threshold level , for the cases of Swerling I-II target, with individual pulse detection, the P(ν) is [23]:

$$P(v)=\frac{1}{1+SNR}exp\left[\frac{-v}{1+SNR}\right], \quad (17)$$

So detection probability P_d of the target is:

$$P_d=exp\left[\frac{-T}{1+SNR}\right], \quad (18)$$

By calculating the probability of detection for the radar receiver in case of using the proposed technique (TVGA), and comparing this results with the probability of detection for the same system but in case of using the old techniques (AGC, IAGC, and STC).

5 Simulation and Results

5.1 ASO/TVGA model simulation

Fig.4 (a), (b), (c) shows the relation between the voltage components $V_1(s)$, $V_2(s)$, and $V_3(s)$, respectively and the frequency. From these Figures it can be found that the voltages were increased by adding the emitter resistance that gives more linearity in design of the TVGA.

Fig.5 shows that the drop in the DC current I_o is reduced as the emitter resistance increases at R_B = 1 MΩ, from this figure we can see that in case of using emitter resistance = 10Ω (ASO/TVGA model) we got the least drop in the DC current compared with the TVGA model without emitter resistance, AGC model, and STC model, so that the IMR3 is decreased and more linearity is achieved using the proposed model.

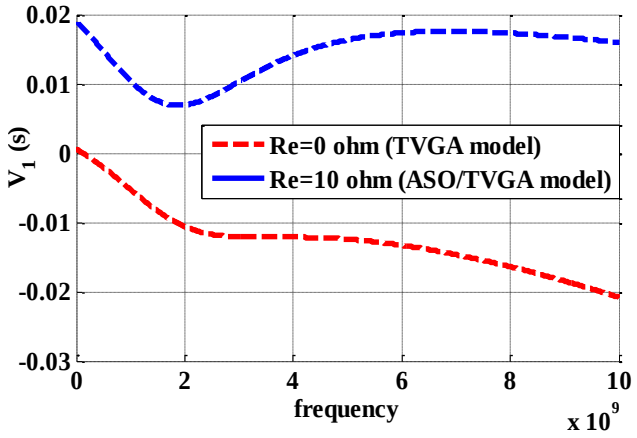

(a)

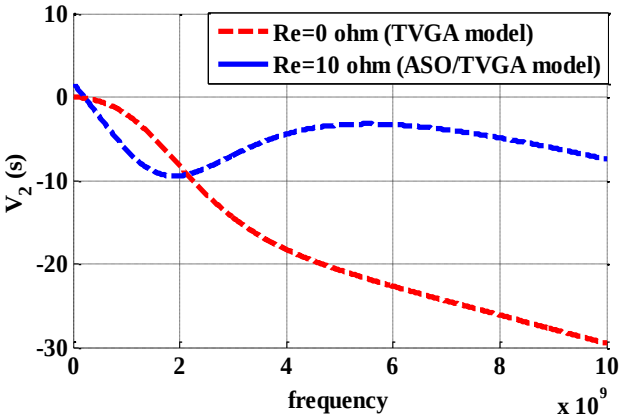

(b)

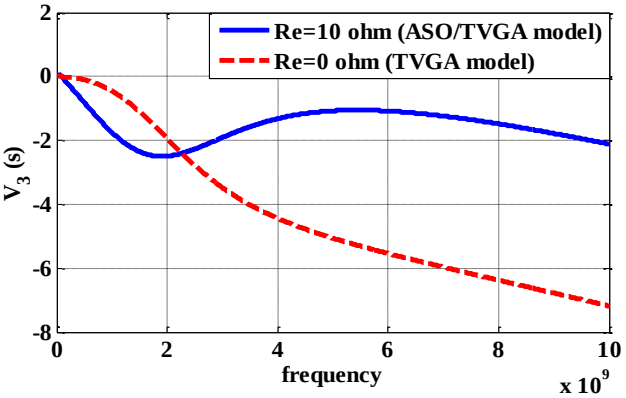

(c)

Fig.4: The function Vi(s) against the frequency for the proposed model (ASO/TVGA) and the previous model (TVGA)

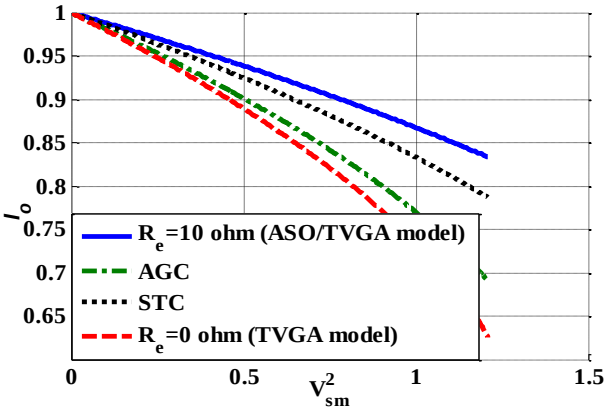

Fig.5: The drop in DC current I_o for the different models

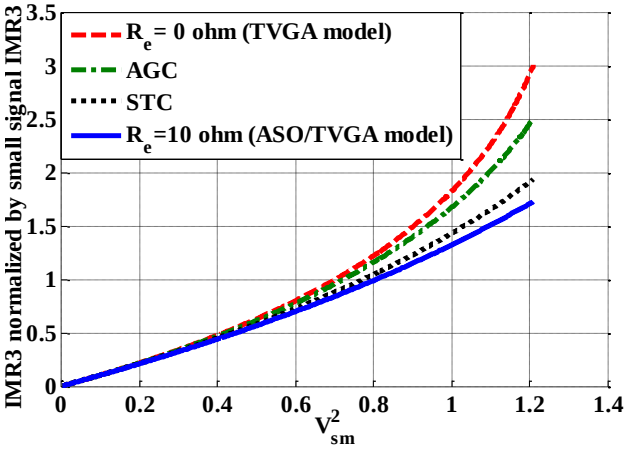

Fig.6: The IMR3 for the different models

From Figs.5, and 6 it can be found that emitter resistance will introduce more linearity by reducing the IMR3 and reducing the drop of the DC current I_o, so if a 10 ohm emitter resistance is inserted in the design of TVGA a more linearity can be found, also more linearity can be introduced as the emitter resistance increases but it affects the gain of the TVGA.

5.1 The Monostatic Radar Model Simulation

Table 1 is listed the design parameters used in the model, Table 2 shows the three stationary, non-fluctuating targets in space, their positions, and radar cross sections.

TABLE 1 DESIGN SPECIFICATIONS

Radar parameter	Value
Probability of detection (P_D)	0.9
probability of false alarm (P_{FA})	10^{-6}
Maximum range R_{max} (m)	6000
Range resolution R_{res} (m)	50
Operating frequency (GHz)	9.3
Receiver and transmitter gain (dB)	30

TABLE 2 TARGETS PARAMETERS

Target number	RCS (m2)	Position (m)
No.1	1	1245
No.2	1	2458
No.3	1	3990

The threshold is increased by the matched filter processing gain, as shown in Fig.7 this figure shows the first received pulse with the threshold before applying matched filter, and the same pulse after passing through the matched filter with the same RCS = 1m2.

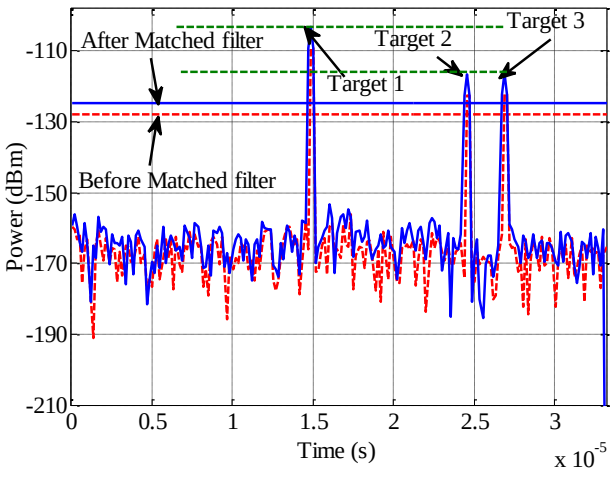

Fig. 7: The first received pulse with the threshold before and after using the matched filter

Also Fig.7 shows two green dashed lines to demonstrate the difference in the power level of the 3 targets due to the range dependent. To ensure that the threshold is fair to all the targets within the detectable range, a time varying gain is applied to compensate for the range dependent loss in the received echo. The time varying gain operation results in a ramp in the noise [24] floor as shown in Fig.8 And also we need to perform pulse integration to ensure the power of returned echoes from the targets can surpass the threshold while leaving the noise floor below the bar.

We can see that there is no difference between the power levels of the three targets, this is due to applying ASO/TVGA to make the power loss compensation and now there is no loss of the power of targets (2, 3) due to range. We can further improve the SNR by noncoherently integrating the received pulses, after the noncoherent integration stage, the data is ready for the final detection stage. We can see that the required power has dropped to around 5 dB. Further reduction of SNR can be achieved by integrating more pulses, but the number of pulses available for integration is normally limited due to the motion of the target or the heterogeneity of the environment [22], [23].

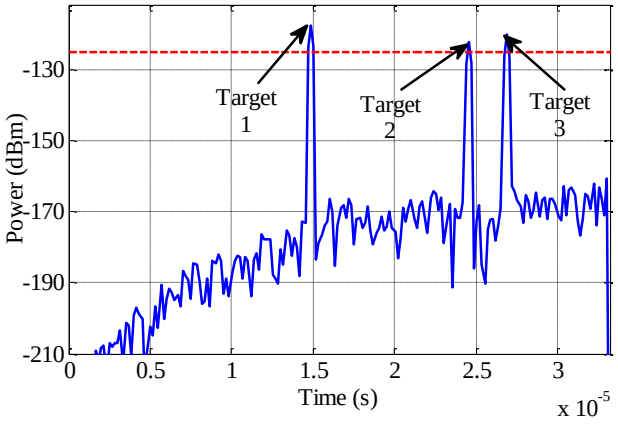

Fig. 8: The first pulse after applying ASO/TVGA and integration of 10 pulses

Now we can apply the simulation for detecting the three targets at different ranges to show that the receiver now has a wide dynamic range after applying the proposed model. Fig.9 shows the results at maximum range of 35 km, it shows that the three targets detected using ASO/TVGA, Fig.10 shows the same results at maximum range of 160 km. Now we can see that ASO/TVGA can be applied at different ranges for improvement of detection, which yields to a wide dynamic range in the monostatic pulsed radar receiver and gives more

sensitivity at different power levels of the received echoes which may vary due to environment effects such as the noise, jamming, and clutter.

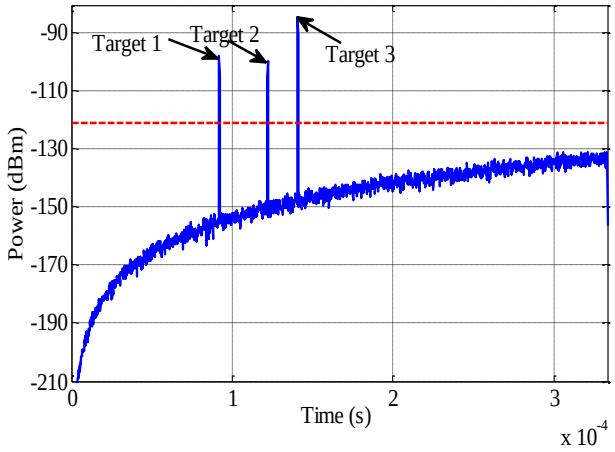

Fig. 9: The first pulse after applying ASO/TVGA at maximum range of 35 km

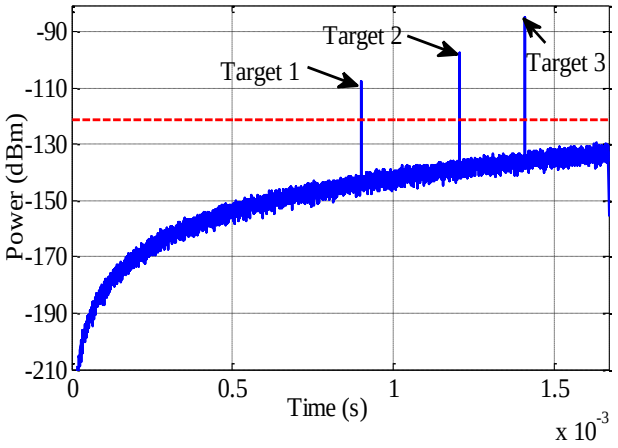

Fig. 10: The first pulse after applying ASO/TVGA at maximum range of 160 km

The true ranges and the estimate ranges of the targets are shown in Table 3.

TABLE 3 RANGE RESULTS

Target number	Estimate range (m)	True range (m)	Range error (m)
No.1	1245	1257	12
No.2	2458	2468	10
No.3	3990	4015	25

We can see that the error in range is very small and within the range resolution limit so we achieved a good resolution in range.

Also the true angles and the estimate angles of the targets are shown in Table 4.

It has been noted that the error in angle estimation is very small and about 0.4 so it gives a good resolution in angle.

TABLE 4 DIRECTION RESULTS

Target number	Estimate angle (degree)	True angle (degree)	Angle error (degree)
No.1	25.9504	25.4137	0.5367
No.2	16.0360	15.8173	0.2187
No.3	6.8892	6.3892	0.5

Also we can find that the probability of detection for the proposed model is higher than the other models, as shown in Fig.11.

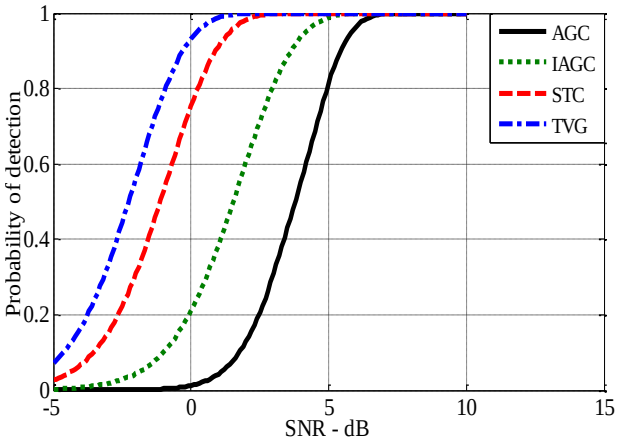

Fig. 11: The probability of detection for the proposed model with the old models

6 Conclusion

In this paper, we have proposed a new adaptive sweep optimization (ASO) technique to increase the linear region for the TVGA in order to have a wide dynamic range for this the radar receiver and increase its sensitivity, this enhancement was achieved by adding the emitter resistance and make tuning for all the amplifier parameters, then we designed a radar system, and applying the ASO on the TVGA, in order to make validation three real targets were detected by the radar after applying ASO/TVGA. The detection scheme identifies the peaks and then translates their positions into the

ranges of the targets. The simulation results showed that the performance of the detector has been improved, also the probability of detection was improved, and the sensitivity of the receiver, and the receiver dynamic range was also increased.

References:

[1] Kanemoto,D., Sato,T., Ohki,M., Muta,O., Fu rukawa,H., linearity enhancement technique for one bit A/D converter in wireless communication devices, *Consumer Electronics (ISCE 2014), The 18th IEEE International*, 2014, pp. 1-2.

[2] Varahram, P. Ali, B.M., Mohammady S., Sulaiman N., Power amplifier linearization scheme to mitigate superfluous radiations and suppress adjacent channel interference, *Communications, IET* , Vol. 8, No. 2, 2014, pp. 258-265.

[3] Benqing Guo, Huifen Wang, Guoning Yang, A Wideband Merged CMOS Active Mixer Exploiting Noise Cancellation and Linearity Enhancement, *Microwave Theory and Techniques, IEEE Transactions on*, Vol. 62, No. 9, 2014, pp. 2084-2091.

[4] Qi N., Fang Y., Ren X., Wu Y., Varying-Gain Modeling and Advanced DMPC Control of an AFM System, *Nanotechnology, IEEE Transactions on*, Vol.14, No. 1, 2015, pp. 82-92.

[5] V. Nagarajan, M.R. Chidambara, R.N. Sharma, New approach to improved detection and tracking performance in track-while-scan radars part 1, introduction and review, *Communications, Radar and Signal Processing, IEE Proceedings*, 1987, Vol. 134, No. 1, pp. 89-92.

[6] Harun Taha Hayvaci, Antonio De Maioy, Danilo Erricolo, Improved Detection Probability of a Radar Target in the Presence of Multipath with Prior Knowledge of the Environment, Radar, Sonar & Navigation, IET, Vol. 7, No. 1, 2013, pp. 36-46.

[7] Jianpeng Fan, Benyuan Liu, Zaiqi Lu, Threshold variation based analysis and implementation of an optimized AGC circuitry for digital IF receiver, *Computer Application and System Modeling (ICCASM) 2010 International Conference*, Vol. 10, 2010, pp. 64-68.

[8] M. Zisserson, Z. Turski, A Wideband Instantaneous Automatic Gain Control Amplifier, *Microwave conference 11th European*, 1981, pp. 787-792.

[9] Xiufeng Song, Shengli Zhou, P. Willett, Enhanced multi static radar resolution via STC, *Radar Conference, IEEE*, 2009, pp. 1-6

[10] Amir Al-Mslmany, Caiyun Wang, Qunsheng Cao, An Analytical Model for Improvement of Linearity andEfficiency of RF Linear Power Amplifiers for Radar Systems, *International Journal of Modeling and Optimization*, Vol. 4, No. 2, 2014, pp. 133-136.

[11] Yao Jiajian, Time-Gain-Compensation Amplifier for Ultrasonic Echo Signal Processing, *Faculty of E.E.M.C.S, Delft University of Technology, in partial fulfillment of MSc. Degree*, 2011.

[12] Schetzen M., The Volterra and Wiener theories of nonlinear systems, Control Theory and Applications", *IEE Proceedings D, New York, John Wiley & Sons*, 1980, Vol. 127, No. 5.

[13] YuanQuan, Wang Zhigong, Li Qin, A 0.35-μm Bi CMOS Automatic Gain Control IF Amplifier for Radar Receivers, *Microwave, Antenna, Propagation and EMC Technologies for Wireless Communications*, 2007, pp. 1375-1378.

[14] Wu Tuo Chen, Hongyi and QianDahong, Theoretical analysis and an improvement method of the bias effect on the linearity of RF linear power amplifiers, *Institute of Microelectronics, Tsinghua University, Beijing 100084*, Vol. 30, No. 5, 2009, pp. 1-7.

[15] M. Malanowski, R. Haugen, M.S.Greco, D.W. O,Hagan, R.Plšek, A, Land and sea clutter from FM-based passive bistatic radars, *Radar, Sonar & Navigation, IET*, Vol. 8, No. 2, 2014, pp. 160-166.

[16] Qi, L., Tao, R., Zhou, S.Y., Detection and parameter estimation of multicomponent LFM signal based on the fractional Fourier transform, *Sci. China Ser F, Inf. Sci*, Vol. 47, No. 2, 2004, pp. 184-198.

[17] Tufts D.W., Cann A.J., On Albersheim,s Detection Equation, *Aerospae and Electronic Systems, IEEE Transactions*, Vol. AES-19, No. 4, 1983, pp. 643-647.

[18] Bassem R. Mahafza, *Simulations for Radar Systems Design*, Decibel Research, Inc. Huntsville, Alabama, 2004, pp. 231-260.

[19] Mark A. Richards, *Fundamentals of Radar Signal Processing*, Georgia institute of technology, 2005, pp. 313-379.

[20] Skolnik, M.I., *Introduction to radar systems*, 3rd edn., McGraw-Hill Book Company, 2001, pp. 192-223.

[21] Djuric, P.M., Kay, S.M., Parameter estimation of chirp signals, *IEEE Trans. Acoust. Speech*

Signal Process., Vol. 38, No. 12, 1990, pp. 2118-2126.

[22] Wehner, D.R., *High-resolution radar*, 2nd edn. Artech House, 1995, pp. 301-309.

[23] Kelly, E.J., Wishner, R.P., Matched-filter theory for high velocity, accelerating targets, *IEEE Trans. Military Electron*., Vol. 9, No. 1, 1965, pp. 56-69.

[24] Abatzoglou, T., Range, radial velocity, and acceleration MLE using radar LFM pulse train, *IEEE Trans. Aerosp. Electron*. Syst, Vol. 34, No. 4, 1998, pp. 1070-1083.